ISSN 1007-9327 (print)
ISSN 2219-2840 (online)

World Journal of *Gastroenterology*

World J Gastroenterol 2020 June 28; 26(24): 3318-3516

Published by Baishideng Publishing Group Inc

World Journal of Gastroenterology

Contents

Weekly Volume 26 Number 24 June 28, 2020

OPINION REVIEW

REVIEW

MINIREVIEWS

ORIGINAL ARTICLE

Basic Study

Retrospective Cohort Study

World Journal of Gastroenterology

Weekly Volume 26 Number 24 June 28, 2020

Contents

ABOUT COVER

Editorial board member of *World Journal of Gastroenterology*, Dr. Ji is a Distinguished Professor in Shanghai University of Traditional Chinese medicine, Shanghai, China. Having received his Bachelor degree from Yangzhou College of medicine in 1991, Dr. Ji undertook his postgraduate training first at Hubei College of Traditional Chinese medicine, received his Master degree in 1994, and then at Shanghai University of Traditional Chinese medicine, received his PhD in 1997. He became Chief Physician in the Gastroenterology Division, Longhua Hospital affiliated to Shanghai University of Traditional Chinese medicine since 2004. His ongoing research interests are applicating Evidence-based medicine methods to study the effects, and managing the disease-syndrome pattern establishment of integrative medicine on digestive diseases. Currently, he is the President of the Shanghai Association for the Study of the Liver with integrative medicine.

AIMS AND SCOPE

The primary aim of *World Journal of Gastroenterology* (*WJG*, *World J Gastroenterol*) is to provide scholars and readers from various fields of gastroenterology and hepatology with a platform to publish high-quality basic and clinical research articles and communicate their research findings online. *WJG* mainly publishes articles reporting research results and findings obtained in the field of gastroenterology and hepatology and covering a wide range of topics including gastroenterology, hepatology, gastrointestinal endoscopy, gastrointestinal surgery, gastrointestinal oncology, and pediatric gastroenterology.

INDEXING/ABSTRACTING

The *WJG* is now indexed in Current Contents®/Clinical Medicine, Science Citation Index Expanded (also known as SciSearch®), Journal Citation Reports®, Index Medicus, MEDLINE, PubMed, PubMed Central, and Scopus. The 2019 edition of Journal Citation Report® cites the 2018 impact factor for *WJG* as 3.411 (5-year impact factor: 3.579), ranking *WJG* as 35th among 84 journals in gastroenterology and hepatology (quartile in category Q2).

RESPONSIBLE EDITORS FOR THIS ISSUE

NAME OF JOURNAL
World Journal of Gastroenterology

ISSN
ISSN 1007-9327 (print) ISSN 2219-2840 (online)

LAUNCH DATE
October 1, 1995

FREQUENCY
Weekly

EDITORS-IN-CHIEF
Andrzej S Tarnawski, Subrata Ghosh

EDITORIAL BOARD MEMBERS
http://www.wjgnet.com/1007-9327/editorialboard.htm

PUBLICATION DATE
June 28, 2020

INSTRUCTIONS TO AUTHORS
https://www.wjgnet.com/bpg/gerinfo/204

GUIDELINES FOR ETHICS DOCUMENTS
https://www.wjgnet.com/bpg/GerInfo/287

GUIDELINES FOR NON-NATIVE SPEAKERS OF ENGLISH
https://www.wjgnet.com/bpg/gerinfo/240

PUBLICATION ETHICS
https://www.wjgnet.com/bpg/GerInfo/288

PUBLICATION MISCONDUCT
https://www.wjgnet.com/bpg/gerinfo/208

ARTICLE PROCESSING CHARGE
https://www.wjgnet.com/bpg/gerinfo/242

STEPS FOR SUBMITTING MANUSCRIPTS
https://www.wjgnet.com/bpg/GerInfo/239

ONLINE SUBMISSION
https://www.f6publishing.com

World Journal of Gastroenterology

Submit a Manuscript: https://www.f6publishing.com

World J Gastroenterol 2020 June 28; 26(24): 3458-3471

DOI: 10.3748/wjg.v26.i24.3458

ISSN 1007-9327 (print) ISSN 2219-2840 (online)

ORIGINAL ARTICLE

Retrospective Cohort Study

Multiphase computed tomography radiomics of pancreatic intraductal papillary mucinous neoplasms to predict malignancy

Stuart L Polk, Jung W Choi, Melissa J McGettigan, Trevor Rose, Abraham Ahmed, Jongphil Kim, Kun Jiang, Yoganand Balagurunathan, Jin Qi, Paola T Farah, Alisha Rathi, Jennifer B Permuth, Daniel Jeong

ORCID number: Stuart L Polk (0000-0001-5225-6970); Jung W Choi (0000-0001-8206-4259); Melissa J McGettigan (0000-0001-9231-8224); Trevor Rose (0000-0003-1513-6069); Abraham Ahmed (0000-0003-3888-238X); Jongphil Kim (0000-0002-7430-2226); Kun Jiang (0000-0001-8531-7813); Yoganand Balagurunathan (0000-0002-5598-4727); Jin Qi (0000-0002-6112-3827); Paola T Farah (0000-0002-7410-4377); Alisha Rathi (0000-0003-3792-885X); Jennifer B Permuth (0000-0002-4726-9264); Daniel Jeong (0000-0002-8893-7687).

Author contributions: Choi JW, Rose T, Ahmed A, McGettigan M, Balagurunathan Y, Qi J, Farah P, Rathi A and Permuth JB contributed to research design and manuscript editing; Rathi A and Jeong D evaluated radiological imaging; Polk SL and Jeong D wrote the paper; all authors contributed to the manuscript content and revisions prior to submission.

Supported by National Cancer Institute of the National Institutes of Health, No. R37CA229810; and Biostatistics Core Facility at the H. Lee Moffitt Cancer Center and Research Institute, an NCI designated Comprehensive Cancer Center, No. P30-CA076292.

Institutional review board statement: The study was reviewed and approved by University of South Florida Institutional Review Board.

Stuart L Polk, University of South Florida College of Medicine, Tampa, FL 33612, United States

Jung W Choi, Melissa J McGettigan, Trevor Rose, Abraham Ahmed, Daniel Jeong, Department of Diagnostic and Interventional Radiology, H. Lee Moffitt Cancer Center and Research Institute, Tampa, FL 33612, United States

Jongphil Kim, Yoganand Balagurunathan, Department of Biostatistics and Bioinformatics, H. Lee Moffitt Cancer Center and Research Institute, Tampa, FL 33612, United States

Kun Jiang, Department of Anatomic Pathology, H. Lee Moffitt Cancer Center and Research Institute, Tampa, FL 33612, United States

Jin Qi, Department of Cancer Physiology, H. Lee Moffitt Cancer Center and Research Institute, Tampa, FL 33612, United States

Paola T Farah, Department of Clinical Science, H. Lee Moffitt Cancer Center and Research Institute, Tampa, FL 33612, United States

Alisha Rathi, Department of Radiology, University of Florida, Gainesville, FL 32610, United States

Jennifer B Permuth, Department of Cancer Epidemiology, H. Lee Moffitt Cancer Center and Research Institute, Tampa, FL 33612, United States

Corresponding author: Daniel Jeong, MD, Associate Professor, Department of Diagnostic and Interventional Radiology, H. Lee Moffitt Cancer Center and Research Institute, 12902 USF Magnolia Dr., Tampa, FL 33612, United States. daniel.jeong@moffitt.org

Abstract

BACKGROUND

Intraductal papillary mucinous neoplasms (IPMNs) are non-invasive pancreatic precursor lesions that can potentially develop into invasive pancreatic ductal adenocarcinoma. Currently, the International Consensus Guidelines (ICG) for IPMNs provides the basis for evaluating suspected IPMNs on computed tomography (CT) imaging. Despite using the ICG, it remains challenging to accurately predict whether IPMNs harbor high grade or invasive disease which would warrant surgical resection. A supplementary quantitative radiological tool, radiomics, may improve diagnostic accuracy of radiological evaluation of IPMNs. We hypothesized that using CT whole lesion radiomics features in

Informed consent statement: Based on the institutional review board approved protocol, patients were not required to give informed consent to this retrospective study because analysis used anonymized data obtained after each patient agreed to treatment by written consent.

Conflict-of-interest statement: The authors declare that they have no conflict of interest.

Data sharing statement: No additional data are available.

STROBE statement: The authors have read the STROBE statement, and the manuscript was prepared and revised according to STROBE guidelines.

Manuscript source: Unsolicited manuscript

Received: December 30, 2019
Peer-review started: January 8, 2020
First decision: February 28, 2020
Revised: May 9, 2020
Accepted: June 13, 2020
Article in press: June 13, 2020
Published online: June 28, 2020

P-Reviewer: Aoki H, Neri V, Zhu JB
S-Editor: Ma YJ
L-Editor: A
E-Editor: Wu YXJ

conjunction with the ICG could improve the diagnostic accuracy of predicting IPMN histology.

AIM

To evaluate whole lesion CT radiomic analysis of IPMNs for predicting malignant histology compared to International Consensus Guidelines.

METHODS

Fifty-one subjects who had pancreatic surgical resection at our institution with histology demonstrating IPMN and available preoperative CT imaging were included in this retrospective cohort. Whole lesion semi-automated segmentation was performed on each preoperative CT using Healthmyne software (Healthmyne, Madison, WI). Thirty-nine relevant radiomic features were extracted from each lesion on each available contrast phase. Univariate analysis of the 39 radiomics features was performed for each contrast phase and values were compared between malignant and benign IPMN groups using logistic regression. Conventional quantitative and qualitative CT measurements were also compared between groups, *via* χ^2 (categorical) and Mann Whitney *U* (continuous) variables.

RESULTS

Twenty-nine subjects (15 males, age 71 ± 9 years) with high grade or invasive tumor histology comprised the "malignant" cohort, while 22 subjects (11 males, age 70 ± 7 years) with low grade tumor histology were included in the "benign" cohort. Radiomic analysis showed 18/39 precontrast, 19/39 arterial phase, and 21/39 venous phase features differentiated malignant from benign IPMNs ($P < 0.05$). Multivariate analysis including only ICG criteria yielded two significant variables: thickened and enhancing cyst wall and enhancing mural nodule < 5 mm with an AUC (95%CI) of 0.817 (0.709-0.926). Multivariable post contrast radiomics achieved an AUC (95%CI) of 0.87 (0.767-0.974) for a model including arterial phase radiomics features and 0.834 (0.716-0.953) for a model including venous phase radiomics features. Combined multivariable model including conventional variables and arterial phase radiomics features achieved an AUC (95%CI) of 0.93 (0.85-1.0) with a 5-fold cross validation AUC of 0.90.

CONCLUSION

Multi-phase CT radiomics evaluation could play a role in improving predictive capability in diagnosing malignancy in IPMNs. Future larger studies may help determine the clinical significance of our findings.

Key words: Radiomics; Intraductal papillary mucinous neoplasm; Multiphase computed tomography; Pancreas; Oncology; Pancreatic cancer

Core tip: When pancreatic intraductal papillary mucinous neoplasms (IPMNs) are detected on computed tomography (CT) imaging, it is difficult to definitively assess whether they possess benign or malignant pathology. Few studies have investigated the capabilities of CT radiomics in predicting malignant pathology in IPMNs. In this retrospective cohort study on preoperative multiphase post contrast CTs in IPMNs, a combined model using radiomics features and International Consensus Guidelines (ICG) had better diagnostic accuracy in predicting malignant pathology than a model using ICG alone.

Citation: Polk SL, Choi JW, McGettigan MJ, Rose T, Ahmed A, Kim J, Jiang K, Balagurunathan Y, Qi J, Farah PT, Rathi A, Permuth JB, Jeong D. Multiphase computed tomography radiomics of pancreatic intraductal papillary mucinous neoplasms to predict malignancy. *World J Gastroenterol* 2020; 26(24): 3458-3471
URL: https://www.wjgnet.com/1007-9327/full/v26/i24/3458.htm
DOI: https://dx.doi.org/10.3748/wjg.v26.i24.3458

INTRODUCTION

Intraductal papillary mucinous neoplasms (IPMNs) are mucin producing neoplasms that can arise from the pancreatic main duct or its side branches. These are considered non-invasive precursor lesions that can give rise to invasive pancreatic ductal adenocarcinoma. IPMNs are a subset of pancreatic cystic lesions that have been shown in histopathological studies to account for approximately half of resected pancreatic cysts[1-3]. IPMNs are typically detected incidentally on imaging, as pancreatic cystic lesions are reported to be present on up to 2.6% of all computed tomography (CT) studies[4,5]. Despite increased detection of IPMNs on CT, it remains challenging to accurately predict whether IPMNs harbor high grade or invasive disease which would warrant surgical resection. Conversely, there exists a significant risk of major or minor post-operative morbidity (40%) and post-operative mortality (2.3%) with surgical resection of pancreatic cystic lesions[6]. This underscores the implications at stake for accurately identifying an IPMN as malignant or benign – it can lead to either the removal of a potentially life-threatening lesion or the avoidance of unnecessary surgical intervention and its associated consequences and economic costs. While the American College of Radiology (ACR), American Gastroenterology Association (AGA) and International Consensus Guidelines (ICG) (also called the Fukuoka Consensus Guidelines, or Fukuoka Criteria) each provide dedicated guidelines for management of cystic pancreatic lesions, no single guideline provides high sensitivity in diagnosing malignant lesions without also causing an increase in false positives[7-9]. At many institutions including ours, the ICG serve as the basis for evaluating suspected IPMNs on imaging[10,11]. ICG includes standard, qualitative radiologic and clinical features categorized as either "worrisome features" or "high-risk stigmata", which are used to classify an IPMN as benign (characterized by low or moderate grade pathology) or malignant (characterized by high grade or invasive pathology). Based on this classification using the ICG criteria, a patient will be designated for surveillance with follow-up in the case of a benign IPMN or further work up and/or surgical resection in the case of a malignant IPMN. CT imaging is important as it provides the basis for standard IPMN evaluation per ICG and allows triaging of patients into intervention or surveillance groups.

Several recent studies have evaluated the accuracy of the ICG 2012 criteria in characterizing IPMNs. Tsukagoshi *et al*[12] reported a diagnostic accuracy of 77% for predicting high *vs* low-grade dysplasia in IPMNs using the ICG criteria. Sugimoto *et al*[13] and Yamada *et al*[14] attained an area under the curve (AUC) of 67% and 63% respectively for predicting malignant *vs* benign IPMNs using the ICG criteria[13,14]. Other studies have illustrated similar diagnostic accuracies in the specificity and positive predictive value (PPV) of the ICG criteria, with false positive rates of up to 47% and 66% in predicting malignancy in branch-duct IPMNs (BD-IPMNs)[7,15,16]. Furthermore, there is a discrepancy between pre- and post-op diagnosis for nearly 1 out of 3 patients who have undergone pancreatic cyst surgery[17]. While the ICG serve as a valuable diagnostic method for characterizing IPMNs, these studies suggest there is still room for improvement. ICG criteria rely heavily on qualitative metrics to predict IPMN pathology. A quantitative radiological assessment, radiomics, may potentially improve diagnostic accuracy of radiological evaluation of IPMNs.

Radiomics involves extraction and analysis of quantitative features from diagnostic images to produce mineable data[18]. Radiomics features encompass size, shape, texture, heterogeneity, and signal intensity. Using dedicated software and predictive models, these imaging features (or radiophenotypes) are quantified into specific numeric values which can be correlated to clinicopathologic diagnoses and outcomes[18]. Radiomic features possess several advantages over standard qualitative radiologic features. They can represent quantitative and objective measures and reflect tumor heterogeneity and sub-regional environment[19,20]. In addition to reproducibility and stability, they also exhibit substantial prognostic value[21-25]. Previous authors have shown that radiomics features can be more strongly linked to outcomes than prevailing clinical data[26-30]. CT is the more common imaging modality for performing radiomics analysis of pancreatic cysts and IPMNs for several reasons. First, CT and magnetic resonance imaging (MRI) display similar accuracy in characterizing pancreatic cysts as either benign or malignant[31,32]. CT also possesses widespread availability, high spatial and temporal resolution, and short scanning durations. Additionally, CT voxels utilize standard Hounsfield Units (HU) and not the relative signal intensity seen with conventional MRI sequences.

Several groups have shown that two dimensional (2D) CT radiomics can help predict malignant histology in IPMNs. Our team showed that a set of textural radiomic features could be used to identify malignant IPMNs with a diagnostic accuracy of 77% using venous phase single mid-lesion images for radiomic analysis[33]. In a related study, Hanania *et al*[34] identified gray level co-occurrence matrix

biomarkers on arterial phase 2D images and achieved a diagnostic accuracy of 82% in predicting malignant or high-grade disease. Chakraborty *et al*[35] used 2D radiomic texture features on venous phase images and reported diagnostic accuracy of 74% in identifying high risk IPMNs. The purpose of this proof-of-concept study is to expand on prior 2D work and to evaluate whole lesion radiomic features of IPMNs in predicting malignant histology on multiphase CT. We hypothesized that CT whole lesion radiomics features in conjunction with the ICG could improve the diagnostic accuracy of predicting IPMN histology.

MATERIALS AND METHODS

Fifty-one subjects with pancreatic lesions who had surgical resection at our tertiary cancer center with histology demonstrating intraductal papillary mucinous neoplasm were included in this IRB approved, Health Insurance Portability and Accountability Act (HIPAA) compliant retrospective cohort. The initial cohort was derived from a radiological records database search with matching pathology result availability. Subjects included had surgical resection between 2001 and 2016 and preoperative multiphase CT available. Subjects were excluded who had only noncontrast or single phase post contrast CT imaging or unavailable pathology reports. Subjects with surgical pathology demonstrating high grade dysplasia or invasive tumor were included in the "malignant" cohort while subjects with surgical pathology demonstrating moderate or low grade dysplasia were included in the "benign" cohort. Benign and malignant cohorts were composed of similar aged subjects with a similar proportion of males and females.

Region identification

Whole lesion semi-automated segmentation was performed on preoperative (within 3 mo preceding surgery) axial CT exams by a dedicated oncologic radiologist, using the HealthMyne software platform (Healthmyne, Madison, WI). CT exams were performed utilizing multiphase protocols and segmentations were performed on each slice of the lesion on all available noncontrast, arterial, and venous phase CTs by a board-certified radiologist (Figure 1). Thirty-nine relevant radiomic features listed in Table 1 were extracted from each segmented lesion and analyzed for each contrast phase.

CT protocols

CT exams were performed on different scanners: Siemens Sensation 16 (n = 29), Sensation 40 (n = 8), Sensation 64 (n = 7), SOMATOM Emotion (n = 1), SOMATOM Definition AS (n = 3), (Siemens Healthcare, Erlangen, Germany). CT exams from GE LightSpeed Pro 32 (n = 1) (GE Healthcare, Waukesha, WI) Philips Brilliance 16P (n = 1) (Philips Medical Systems, Best, The Netherlands), and Toshiba Aquilion (n = 1) (Toshiba Medical Systems Co, Otawara, Japan) were also used for exams in this study. CT exams were 3 phase studies with noncontrast, arterial, and venous phases obtained. Arterial phase CTs were generally obtained with bolus triggering and an injection rate of 4 mL/s of Iopamidol 76% weight based dosing to achieve late arterial phase imaging approximately 35 s post injection (Bracco Diagnostics Inc., Monroe Township, NJ). Venous phase CTs achieved imaging approximately 60 s post injection. Weight based Iopamidol dosing generally ranged from 75 mL for patients below 55 kg, to 150 mL for patients above 110 kg with gradient increases every 5 kg. Field of view (FOV) ranged from (293-494) mm × (293-494) mm for each phase based on patient size. Matrix was 512 × 512 for each CT. Slice thickness was 4.2 ± 1.2 mm for noncontrast exams, and 3.0 ± 0.4 mm for arterial and venous exams. Noncontrast, arterial, and venous phase voxel volumes were 2.5 ± 0.8 mm^3, 1.8 ± 0.5 mm^3, and 1.8 ± 0.5 mm^3, respectively. Region of Interest (ROI) measurements were performed to measure Hounsfield units over the abdominal aorta and suprarenal inferior vena cava (IVC) on each contrast phase to ensure no differences between groups were specifically attributable to contrast phase variability. For contrast phase control purposes, manual regions of interest were drawn over the aorta and IVC and Hounsfield units were recorded to ensure there were no significant differences in contrast phase related variability between groups (Table 2).

Statistical analysis

Univariate analysis of the 39 radiomic features was performed for the pre-contrast, arterial, and venous phase radiomics data. Conventional quantitative and qualitative CT measurements were collected, which included ICG criteria. Categorical variables were compared with the chi-square test and continuous variables compared with the Mann Whitney U test. Logistic regression analysis was performed to discriminate

Table 1 Radiomic features evaluated in the intraductal papillary mucinous neoplasm study cohort (*n* = 39)

HU based features	Length features	Shape features	GLCM features
Mean HU	Volumetric length	Surface area volume	GLCM row mean
Minimum HU	Craniocaudal length	Surface area to volume ratio	GLCM row variance
Maximum HU	Transverse length	Compactness 1st order	GLCM row standard deviation
Median HU	Anterior-posterior length	Compactness 2nd order	GLCM column means
Variance HU		Spherical disproportion	GLCM column variance
Standard deviation HU		Sphericity	GLCM column standard deviation
Root mean square HU			GLCM correlation
Energy HU			GLCM energy
Entropy HU (histogram)			GLCM entropy
Kurtosis HU (histogram)			GLCM contrast
Skewness HU (histogram)			GLCM homogeneity
Mean deviation HU			GLCM dissimilarity
Uniformity HU			GLCM angular second moment
Normalized above mean deviation HU			
Uniformity			

HU: Hounsfield units; GLCM: Gray level co-occurrence matrix.

pathologically-confirmed malignant and benign IPMN case groups using SAS/STAT version 14.3 (SAS Institute Inc., Cary, NC, United States). Multivariate analysis was performed on data normalized by standard deviation to generate a model including radiomic features and clinical variables. Log 2 transformation was performed on 13 radiomic features prior to model building to approximately conform to normality. Features with P values < 0.1 were considered to build multivariable models. Backward elimination was performed with stay level of 0.05. The multivariate model's ability to discriminate was assessed by 5-fold cross validation. The statistical methods of this study were reviewed by our biostatician Jongphil Kim PhD. from H. Lee Moffitt Cancer Center.

RESULTS

The IPMN study cohort consisted of 51 patient subjects. Twenty-nine subjects (15 males, age 71.4 ± 8.6 years) comprised the malignant cohort, and 22 subjects (11 males, age 70.0 ± 7.1 years) comprised the benign cohort. Radiomic analysis showed 18/39 noncontrast (Table 3), 19/39 arterial phase (Table 4), and 21/39 venous phase (Table 5) features differentiated malignant from benign IPMNs (P < 0.05). The most statistically predictive features in univariate analysis were seen on the venous phase and these included log2 (GLCM_energy), log2 (energy_HU), log2 (GLCM_angular_second_moment), and GLCM_entropy.

Of the conventional CT measurements including ICG criteria (Table 6), main pancreatic duct diameter (P < 0.001), enhancing solid component (P = 0.005), and maximum cyst wall thickness (P < 0.001) were the specific features with the most significant difference between malignant and benign pathology groups. Multivariate analysis *via* backward elimination, including the individual ICG 2017 criteria yielded two significant variables: thickened and enhancing cyst wall and enhancing mural nodule < 5 mm with a combined ICG model AUC (95%CI) of 0.817 (0.709-0.926).

Multivariable analysis *via* backward elimination for post contrast radiomics achieved an AUC (95%CI) of 0.87 (0.767-0.974) for a model including arterial phase radiomics features and 0.834 (0.716-0.953) for a model including venous phase radiomics features. Combined multivariable analysis including ICG criteria and radiomic results are shown in Table 7. Of note, the multivariable model including conventional variables and arterial phase radiomics features achieved an AUC (95%CI) of 0.93 (0.85-1.0) with a 5-fold cross validation AUC of 0.90.

No significant differences were noted between malignant and benign cohorts with voxel volumes on noncontrast, arterial, and venous phases (P = 0.5, 0.3, and 0.3) respectively. No significant differences were noted between aortic and IVC ROI Hounsfield unit measurements between groups on each phase (Table 2).

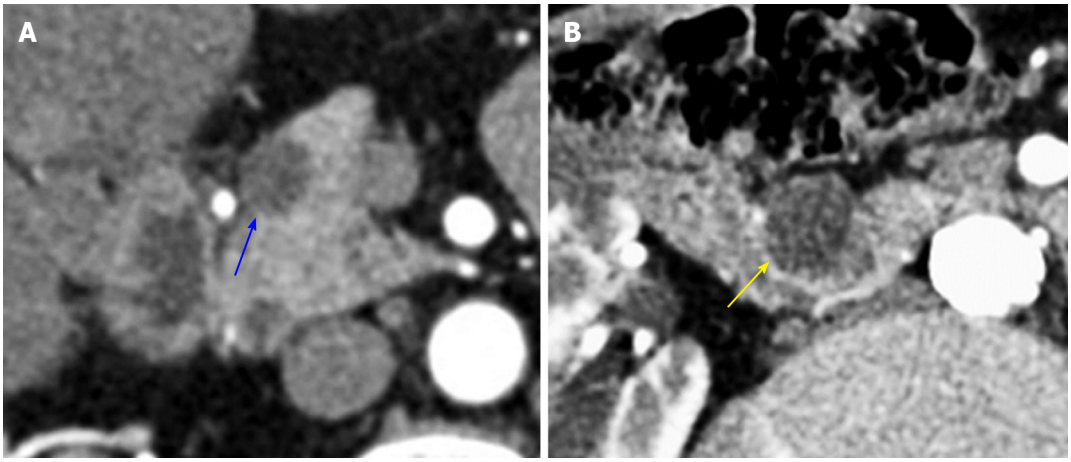

Figure 1 Low and high grade intraductal papillary mucinous neoplasms on computed tomography. A: Axial post contrast arterial phase computed tomography (CT) image magnified at the pancreatic head shows a hypodense well defined pathology proven intraductal papillary mucinous neoplasm (IPMN) with low grade dysplasia (blue arrow). Arterial gray level co-occurrence matrix (GLCM) entropy was 9.31; B: Axial post contrast arterial phase CT image in a different patient with pathology proven IPMN with high grade dysplasia (yellow arrow). Arterial GLCM entropy was 11.52. These lesions could be described similarly using qualitative terminology, however in this study, quantitative radiomics features improved prediction of malignant pathology compared to conventional measures alone.

DISCUSSION

In this retrospective analysis of CT data from patients who underwent resection for IPMN, we demonstrated that a model combining radiomic features and ICG criteria improved diagnostic accuracy compared to ICG criteria alone. Our model yielded an AUC of 0.90 in predicting pathologic status of IPMNs compared to an AUC of 0.82 using the ICG criteria.

Our work is concordant with previous studies by our team and others, attaining similar values of AUC for predicting IPMN malignancy using CT radiomic features[33,34]. Permuth *et al*[33] integrated worrisome radiologic features from the ICG, radiomic features, and miRNA expression levels into a logistic regression model that demonstrated an AUC = 0.93 for predicting IPMN malignant pathology. Hanania *et al*[34] used a cross-validated panel consisting of 10 top-performing markers to attain a linear regression model yielding an AUC = 0.96 for differentiating low-grade and high-grade IPMNs. In line with our study, each of these studies independently identified that the strongest radiomic features for differentiating high-grade and low-grade IPMNs were textural. In a more recent study, Chakraborty *et al*[35] combined radiomic features with five clinical variables associated with IPMN risk to design a predictive model for discriminating between low-risk and high-risk BD-IPMNs, which achieved an AUC = 0.81. The current study adds to these previous works by employing 3D whole lesion analysis as opposed to 2D mid-lesion analysis, and we also evaluated multiphase CT for our radiomic analysis as opposed to solely venous or arterial phase CT. We showed that unique data is contained within radiomics features of each contrast phase. While several individual venous phase features produced the highest univariate AUCs, multivariable analysis showed the arterial phase model had higher multivariable AUC. Our results suggest there is diagnostic benefit in multiphase radiomics evaluation of IPMNs compared solely to venous phase evaluation.

Radiomics allowed us to quantify the appearance of a lesion, which can sometimes be challenging to appreciate qualitatively. We quantified this appearance using entropy applied to the gray level co-occurrence matrix, which is an imaging biomarker that can be used for characterizing tumor phenotype and heterogeneity. Tumors have extensive genetic and phenotypic variation, which manifests as heterogeneity within the same tumor, across metastases from the same tumor, and between patients[36-41]. Entropy reflects tumor heterogeneity and is associated with the extent of differential gene expression within a tumor as well as tumor metabolism, tumor stage, patient prognosis, and treatment response[36-41]. Higher tumor heterogeneity has been associated with poor prognosis, high-grade dysplasia, and resistance to anticancer treatment[42-46]. Tumor heterogeneity can be accurately estimated through genomic analysis, which typically requires invasive and risky tumor biopsies limited to the sampling site, and may not be representative of the entire tumor[42-46]. Radiomics can provide an alternative noninvasive and effective approach to measuring tumor heterogeneity.

In our study, IPMNs with pathology of high-grade dysplasia or invasive disease

Table 2 Computed tomography Hounsfield units measured in the intraductal papillary mucinous neoplasm study cohort by contrast phase

	Benign	Malignant	*P* value
	n = 22	*n* = 29	
Hounsfield units			
Noncontrast aorta	41 ± 6	42 ± 6	0.38
Noncontrast IVC	40 ± 7	40 ± 6	0.85
Arterial phase aorta	322 ± 62	311 ± 70	0.64
Arterial phase IVC	71 ± 30	68 ± 43	0.50
Venous phase aorta	152 ± 30	144 ± 26	0.37
Venous phase IVC	116 ± 30	118 ± 35	0.97

IVC: Inferior vena cava.

had significantly higher gray level co-occurrence matrix (GLCM) features on CT including energy and entropy. GLCM evaluates the spatial distribution of voxels based on their gray levels or in the case of CT, Hounsfield units. In GLCM, a matrix is constructed quantifying how often voxels with each HU value neighbor other voxels with similar HU. Various calculations can be performed on this matrix which ultimately describes the texture of the voxels within a region. Increased entropy as seen in our malignant cohort, suggests a higher degree of underlying tumor heterogeneity and is therefore associated with higher grade tumors. Qualitatively, higher entropy at a macroscopic level correlates with a "salt and pepper" appearance on CT. There are also underlying histologic implications as seen in (Figure 2), where a higher grade IPMN is shown to have more histologic irregularities compared to a lower grade IPMN. The measurement of entropy with quantitative imaging provides a way to appraise the degree of tumor heterogeneity in pancreatic cancer precursors, and elucidates information in the image which would be difficult to describe using only ICG and conventional imaging descriptors.

Despite the benefit that radiomics presents to diagnostic medicine, there are challenges concerning methodology and its implementation into clinical practice that must be addressed. First, CT image fields of view are obtained using different settings based on patient body habitus. This can create voxel sizes that vary between patients, which could affect texture features. While digital imaging and communications in medicine (DICOM) datasets can be normalized for pixel size homogeneity, this was not performed in our series. However, we calculated voxel volumes for each CT based on FOV, matrix, and slice thickness data for our cohort and saw no significant differences between groups related to voxel size inhomogeneity. Additionally, multiphase post-contrast abdominal CT involves imaging at standardized times after contrast injection; however, imaging presentation can be sensitive to a patient's cardiac output[47]. The varied times of arrival of contrast to a lesion may slightly alter the post contrast Hounsfield Units, and therefore the quantification of radiomic features in that lesion. We performed standardized ROI Hounsfield measurements of the aorta and IVC on each of the 3 contrast phases and showed there was no significant contrast timing difference affecting our cohorts in each phase.

It is also important to normalize radiomic variables to a uniform scale when working with models. We performed this for multivariate analysis by normalizing feature values by standard deviations so that all variables are on a constant scale similar to previous authors[48]. Additionally, logarithmic standardization may be helpful to reduce the effect of statistical outliers. Degrees of change within each radiomic feature are relative to the group's composition and there are no well-established normal ranges for radiomic values within pancreatic IPMNs. Furthermore, radiomic feature nomenclature can vary depending on techniques and available software, highlighting the need for standard operating procedures and universal language in cases of collaboration between different practices, providers, and institutions[49].

Limitations of this proof-of-concept study include its retrospective study design and small sample size. We acknowledge that the main criteria for inclusion were a pathologic diagnosis obtained through surgical resection, which makes the study vulnerable to selection bias. In radiomic studies involving many features and/or biomarkers, it is more ideal to have a large sample size for logistic regression analysis. Also, performing radiomics on post-contrast CT is sensitive to slight changes in

Table 3 Noncontrast phase radiomics features ($P < 0.05$) for the intraductal papillary mucinous neoplasm study cohort

Variables	SD	*P* value	OR per 1 SD increase	95%CI lower	Upper	AUC (95%CI)
Log2 (energy_HU)	2.511	0.002	4.33	1.69	11.11	0.82 (0.689-0.951)
Median_HU	10.72	0.003	4.43	1.65	11.85	0.794 (0.658-0.929)
Log2 (GLCM_row_mean)	1.129	0.007	9.21E+39	8.82E+10	9.62E+68	0.785 (0.648-0.923)
Root_mean_square	10.38	0.011	8.03	1.61	40	0.779 (0.641-0.917)
Mean_HU	11.22	0.006	3.73	1.47	9.46	0.773 (0.631-0.916)
Log2 (surface_area_mm^2)	1.592	0.006	3.18	1.4	7.22	0.765 (0.613-0.918)
Volumetric_length_mm	25.05	0.007	4.46	1.5	13.26	0.759 (0.602-0.916)
Compactness2_mm	0.144	0.017	0.38	0.17	0.84	0.749 (0.59-0.908)
Sphericity_mm	0.076	0.034	0.39	0.17	0.93	0.749 (0.59-0.908)
Transverse_length_mm	18.14	0.012	2.99	1.28	6.98	0.741 (0.585-0.896)
GLCM_entropy	1.642	0.01	3.04	1.31	7.05	0.737 (0.581-0.893)
Log2 (GLCM_energy)	0.764	0.011	0.33	0.14	0.78	0.735 (0.581-0.889)
Log2 (GLCM_ASM)	1.527	0.011	0.33	0.14	0.78	0.735 (0.581-0.889)
Compactness1_mm	30.29	0.047	2.27	1.02	5.05	0.729 (0.568-0.89)
Antpost_length_mm	15.85	0.04	2.35	1.04	5.3	0.715 (0.55-0.879)
Log2 (max_HU)	1.043	0.043	2.94	1.04	8.28	0.712 (0.559-0.864)
Surface_area_to_volume_ratio_mm	0.2	0.019	0.38	0.17	0.84	0.694 (0.527-0.862)
Cranialcaudal_length_mm	14.55	0.043	2.03	1.03	4	0.687 (0.521-0.854)

SD: Standard deviation; OR: Odds ratio; CI: Confidence interval; AUC: Area under the curve; HU: Hounsfield units; GLCM: Gray level co-occurrence matrix; ASM: Angular second moment; Max: Maximum.

timing, causing variability in the quality of the images generated. To a similar point, since it is critical that CT scanner settings be homogenous for radiomics analysis, another limitation to this study is heterogeneity in CT scanner type and settings, as there is known radiomics variability with different scanner settings[49,50]. Our study included CT scans across a relatively long period involving different available CT technologies, whereas a future evaluation could be limited to a single scanner or provide inter-scanner validation. Furthermore, our study included both main-duct and branch-duct IPMNs. Main-duct IPMNs possess a much higher risk of malignant progression than branch-duct IPMNs, and are typically designated directly for surgery regardless of diagnostic evaluation of malignant status[51]. Therefore, future larger prospective radiomics studies evaluating particularly branch-duct IPMNs may have greater implications on management.

In summary, this study demonstrates the potential utility of whole lesion 3D radiomics as a supplementary method for predicting IPMN malignancy. Our findings suggest that utilizing radiomic features in combination with ICG criteria to evaluate IPMN pathology on CT can improve accuracy in prediction of high- or low-grade tumor histology. Additionally, multi-phase post contrast CT radiomic analysis may have diagnostic benefits over single venous phase CT analysis. We have just started to conduct a larger multi-center radiomic study that will have a training and test cohort and an independent prospective validation cohort and will integrate blood-based biomarker data to allow earlier and more accurate diagnosis of IPMNs of concern. As a result, patients may receive earlier surgical intervention when warranted and avoid unnecessary interventions in the cases of low risk disease.

Table 4 Arterial phase radiomics features ($P < 0.05$) for the intraductal papillary mucinous neoplasm study cohort

Variables	SD	*P* value	OR per 1 SD increase	95%CI lower	Upper	AUC (95%CI)
Log2 (energy_HU)	2.588	0.002	4.14	1.69	10.14	0.806 (0.674-0.937)
Log2 (max_HU)	1.002	0.008	4.13	1.46	11.72	0.787 (0.648-0.927)
Log2 (GLCM_energy)	0.778	0.007	0.28	0.11	0.7	0.775 (0.635-0.915)
Log2 (GLCM_ASM)	1.555	0.007	0.28	0.11	0.7	0.775 (0.635-0.915)
GLCM_entropy	1.666	0.007	3.42	1.41	8.29	0.769 (0.624-0.914)
Entropy_HU	0.319	0.007	3.01	1.36	6.66	0.763 (0.619-0.907)
Compactness2_mm	0.15	0.015	0.32	0.13	0.8	0.749 (0.598-0.900)
Sphericity_mm	0.081	0.023	0.3	0.11	0.85	0.749 (0.598-0.900)
Spherical_disproportion_mm	0.14	0.038	3.78	1.08	13.24	0.749 (0.598-0.900)
Root_mean_square	14.8	0.012	4.21	1.38	12.88	0.747 (0.604-0.890)
Log2 (GLCM_row_mean)	0.983	0.028	4.16E+17	106.87	1.62E+33	0.726 (0.575-0.877)
Log2 (surface_area_mm^2)	1.624	0.012	2.63	1.24	5.57	0.721 (0.554-0.888)
Volumetric_length_mm	26.97	0.049	2.62	1.01	6.78	0.721 (0.554-0.888)
Transverse_length_mm	18.4	0.03	2.61	1.1	6.18	0.719 (0.556-0.881)
Mean_HU	16.22	0.022	2.62	1.15	5.96	0.715 (0.561-0.869)
Median_HU	15.71	0.026	2.56	1.12	5.82	0.712 (0.557-0.867)
Log2 (GLCM_col_mean)	0.896	0.038	5.04E+12	5.51	4.61E+24	0.696 (0.539-0.854)
Surface_area_to_volume_ratio_mm	0.19	0.032	0.43	0.2	0.93	0.672 (0.496-0.848)
Mean_deviation_HU	4.72	0.042	2.24	1.03	4.85	0.668 (0.507-0.829)

SD: Standard deviation; OR: Odds ratio; CI: Confidence interval; AUC: Area under the curve; HU: Hounsfield units; GLCM: Gray level co-occurrence matrix; ASM: Angular second moment.

Table 5 Venous phase radiomics features ($P < 0.05$) for the intraductal papillary mucinous neoplasm study cohort

Variables	SD	*P* value	OR per 1 SD increase	95%CI lower	Upper	AUC(95%CI)
Log2 (GLCM_energy)	0.805	0.006	0.28	0.11	0.69	0.836 (0.717-0.955)
Log2 (energy_HU)	2.575	0.002	4.46	1.75	11.37	0.834 (0.716-0.953)
Log2 (GLCM_angular_ second_moment)	1.609	0.006	0.28	0.11	0.7	0.834 (0.714-0.954)
GLCM_entropy	1.709	0.006	3.53	1.44	8.63	0.822 (0.703- 0.941)
Log2 (max_HU)	0.832	0.019	4.57	1.29	16.17	0.762 (0.613-0.911)
Entropy_HU	0.379	0.016	2.5	1.19	5.26	0.757 (0.616-0.899)
Transverse_length_mm	18.85	0.018	2.78	1.19	6.48	0.743 (0.588-0.898)
Log2 (surface_area_mm^2)	1.639	0.012	2.67	1.25	5.73	0.735 (0.574-0.895)
Volumetric_length_mm	26.82	0.028	3.01	1.13	7.99	0.731 (0.565-0.897)
Antpost_length_mm	16.65	0.049	2.28	1.01	5.18	0.729 (0.565-0.893)
Log2 (GLCM_row_var)	0.766	0.04	2.33	1.04	5.2	0.709 (0.554-0.863)
GLCM_row_SD	10.69	0.042	2.99	1.05	8.55	0.709 (0.554-0.863)
Log2 (variance_HU)	0.765	0.04	2.33	1.04	5.19	0.707 (0.552-0.861)
SD_HU	10.68	0.042	2.98	1.04	8.52	0.707 (0.552-0.861)
Cranialcaudal_length_mm	16.91	0.047	2.05	1.01	4.14	0.706 (0.543-0.868)
Log2 (GLCM_col_var)	0.758	0.026	2.57	1.13	5.84	0.705 (0.549-0.86)
Surface_area_to_volume_ratio_mm	0.204	0.042	0.42	0.18	0.96	0.705 (0.54-0.869)
GLCM_col_SD	11.37	0.032	2.89	1.1	7.55	0.702 (0.547-0.858)
Root_mean_square	19.63	0.045	2.18	1.02	4.66	0.702 (0.543-0.862)
Mean_deviation_HU	6.058	0.041	2.11	1.03	4.32	0.696 (0.539-0.853)
GLCM_correlation	0.099	0.027	2.19	1.1	4.38	0.684 (0.527-0.841)

SD: Standard deviation; OR: Odds ratio; CI: Confidence interval; AUC: Area under the curve; GLCM: Gray level co-occurrence matrix; HU: Hounsfield units; VAR: Variance; COL: Column.

Table 6 Distribution of International Consensus Guidelines criteria in benign *vs* malignant intraductal papillary mucinous neoplasm cases

	Benign	Malignant	*P* value
	n = 22	*n* = 29	
Morphology (duct)			
Main/mixed	2	17	< 0.001
Side branch	20	12	< 0.001
High risk stigmata (1 or more)	3	18	< 0.001
Enhancing solid component > 5 mm	3	15	0.005
Main duct ≥ 10 mm	0	5	0.04
Obstructive jaundice	0	1	0.379
Worrisome features (1 or more)	10	28	< 0.001
Cyst ≥ 3 cm	7	21	0.004
Thickened enhancing cyst wall	2	11	0.019
Enhancing mural nodule < 5 mm	2	10	0.034
Main pancreatic duct 5-9 mm	3	12	0.039
Lymphadenopathy	1	12	0.003
Abrupt change in caliber of pancreatic duct with distal atrophy	1	4	0.445
Cyst growth rate ≥ 5 mm in two years			NA[1]
Elevated Ca19-9	3/14	8/24	0.557

[1]Adequate historical imaging was widely unavailable.

Table 7 Multivariable model analysis

Model	Included features	Feature category	*P* value	AUC of model (95%CI)
ICG	Thickened enhancing cyst wall	ICG	0.001	0.817 (0.709-0.926)
	Enhancing mural nodule < 5 mm	ICG	0.048	
Arterial phase radiomics	Log2 (GLCM_col_mean)	Arterial	0.009	0.871 (0.767--0.974)
	GLCM_entropy	Arterial	0.002	
Venous phase radiomics	Log2 (energy_HU)	Venous	0.002	0.834 (0.716-0.953)
Combined model	High risk stigmata (1 or more)	ICG	0.022	0.927 (0.851–1.000)
	Log2 (GLCM_col_mean)	Arterial	0.011	
	GLCM_entropy	Arterial	0.014	

Features with *P* value of < 0.1 were considered to build multivariable models. Based on these features, backward elimination method (stay level of 0.05), the listed features remained within each model. AUC: Area under the curve; CI: Confidence interval; ICG: International Consensus Guidelines; GLCM: Gray level co-occurrence matrix; COL: Column; HU: Hounsfield units.

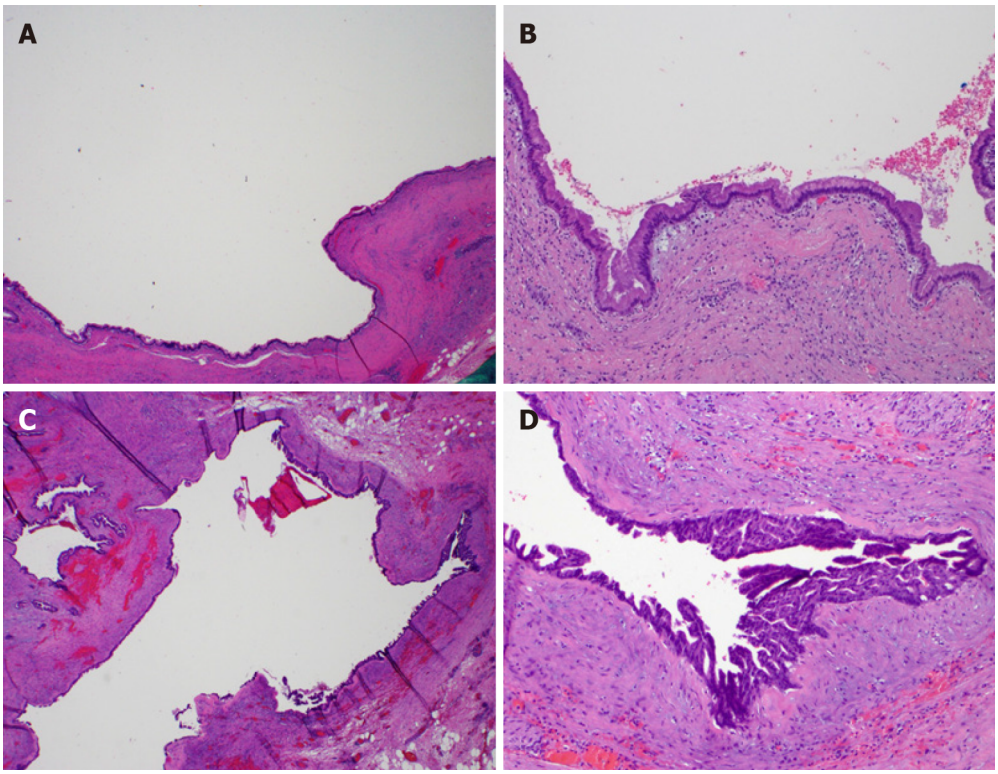

Figure 2 Histology of low grade and high grade intraductal papillary mucinous neoplasm lesions are shown. A: Low grade intraductal papillary mucinous neoplasm (IPMN) hematoxylin and eosin stain (HE) at 20 × magnification; B: Low grade IPMN HE at 100 × magnification. Low grade IPMN is represented by a single layer of mucinous epithelium containing columnar, palisading nuclei and abundant mucinous cytoplasm, with low nuclei/cytoplasmic ratio, minimal cytologic atypia and an absence of obvious mitosis; C: High grade IPMN HE at 20 × magnification; D: High grade IPMN HE at 100 × magnification. In contrast to low grade, high grade IPMN frequently demonstrates decreased cytoplasmic mucin contents, loss of nuclear polarity with nuclear overlapping, higher nuclei/cytoplasmic ratio, significant cytologic atypia and easily identifiable mitosis.

ARTICLE HIGHLIGHTS

Research background

Intraductal papillary mucinous neoplasms (IPMNs) are non-invasive pancreatic precursor lesions which can potentially develop into invasive pancreatic adenocarcinoma. IPMNs are detected on up to 2.6% of all computed tomography (CT) exams, however accurate risk stratification of these lesions remains a challenge.

Research motivation

International Consensus Guidelines (ICG) provides the basis for which pancreatic IPMNs are often evaluated and risk stratified. However, previous studies show limited diagnostic accuracy of ICG criteria in predicting the presence of high grade or invasive disease within an IPMN.

Research objectives

This study aimed to evaluate the diagnostic accuracy of multiphase CT radiomics in predicting malignant *vs* benign IPMN histology.

Research methods

This retrospective cohort study evaluated presurgical whole lesion CT radiomics features on three contrast phases (precontrast, arterial, and venous phases) in patients who underwent surgical resection for IPMN.

Research results

Radiomic analysis showed that 18/39 precontrast, 19/39 arterial phase, and 21/39 venous phase features differentiated malignant from benign IPMNs ($P < 0.05$). Multivariate analysis of ICG criteria alone achieved an AUC (95%CI) of 0.817 (0.709-0.926). A combined multivariable model including conventional variables and arterial phase radiomics features achieved an AUC (95%CI) of 0.93 (0.85-1.0) with a 5-fold cross validation AUC of 0.90.

Research conclusions

Combining multiphase radiomic CT evaluation with conventional ICG criteria analysis may improve predictive capability in diagnosing malignancy in IPMNs.

Research perspectives

This study demonstrates the potential utility of whole lesion radiomics on multiphase CT as a supplementary method for predicting malignancy in IPMN. A larger prospective multi-center trial will be beneficial to further define clinical utility and to improve risk stratification in IPMN.

REFERENCES

1 **Law JK**, Hruban RH, Lennon AM. Management of pancreatic cysts: a multidisciplinary approach. *Curr Opin Gastroenterol* 2013; **29**: 509-516 [PMID: 23872487 DOI: 10.1097/MOG.0b013e328363e3b3]

2 **Spinelli KS**, Fromwiller TE, Daniel RA, Kiely JM, Nakeeb A, Komorowski RA, Wilson SD, Pitt HA. Cystic pancreatic neoplasms: observe or operate. *Ann Surg* 2004; **239**: 651-7; discussion 657-9 [PMID: 15082969 DOI: 10.1097/01.sla.0000124299.57430.ce]

3 **Valsangkar NP**, Morales-Oyarvide V, Thayer SP, Ferrone CR, Wargo JA, Warshaw AL, Fernández-del Castillo C. 851 resected cystic tumors of the pancreas: a 33-year experience at the Massachusetts General Hospital. *Surgery* 2012; **152**: S4-12 [PMID: 22770958 DOI: 10.1016/j.surg.2012.05.033]

4 **Campbell NM**, Katz SS, Escalon JG, Do RK. Imaging patterns of intraductal papillary mucinous neoplasms of the pancreas: an illustrated discussion of the International Consensus Guidelines for the Management of IPMN. *Abdom Imaging* 2015; **40**: 663-677 [PMID: 25219664 DOI: 10.1007/s00261-014-0236-4]

5 **Hoffman DH**, Ream JM, Hajdu CH, Rosenkrantz AB. Utility of whole-lesion ADC histogram metrics for assessing the malignant potential of pancreatic intraductal papillary mucinous neoplasms (IPMNs). *Abdom Radiol (NY)* 2017; **42**: 1222-1228 [PMID: 27900458 DOI: 10.1007/s00261-016-1001-7]

6 **Kleeff J**, Michalski C, Kong B, Erkan M, Roth S, Siveke J, Friess H, Esposito I. Surgery for cystic pancreatic lesions in the post-sendai era: a single institution experience. *HPB Surg* 2015; **2015**: 847837 [PMID: 25873753 DOI: 10.1155/2015/847837]

7 **Xu MM**, Yin S, Siddiqui AA, Salem RR, Schrope B, Sethi A, Poneros JM, Gress FG, Genkinger JM, Do C, Brooks CA, Chabot JA, Kluger MD, Kowalski T, Loren DE, Aslanian H, Farrell JJ, Gonda TA. Comparison of the diagnostic accuracy of three current guidelines for the evaluation of asymptomatic pancreatic cystic neoplasms. *Medicine (Baltimore)* 2017; **96**: e7900 [PMID: 28858107 DOI: 10.1097/MD.0000000000007900]

8 **Megibow AJ**, Baker ME, Morgan DE, Kamel IR, Sahani DV, Newman E, Brugge WR, Berland LL, Pandharipande PV. Management of Incidental Pancreatic Cysts: A White Paper of the ACR Incidental Findings Committee. *J Am Coll Radiol* 2017; **14**: 911-923 [PMID: 28533111 DOI: 10.1016/j.jacr.2017.03.010]

9 **Scheiman JM**, Hwang JH, Moayyedi P. American gastroenterological association technical review on the diagnosis and management of asymptomatic neoplastic pancreatic cysts. *Gastroenterology* 2015; **148**: 824-48.e22 [PMID: 25805376 DOI: 10.1053/j.gastro.2015.01.014]

10 **Tanaka M**, Fernández-del Castillo C, Adsay V, Chari S, Falconi M, Jang JY, Kimura W, Levy P, Pitman MB, Schmidt CM, Shimizu M, Wolfgang CL, Yamaguchi K, Yamao K; International Association of Pancreatology. International consensus guidelines 2012 for the management of IPMN and MCN of the pancreas. *Pancreatology* 2012; **12**: 183-197 [PMID: 22687371 DOI: 10.1016/j.pan.2012.04.004]

11 **Tanaka M**, Fernández-Del Castillo C, Kamisawa T, Jang JY, Levy P, Ohtsuka T, Salvia R, Shimizu Y, Tada M, Wolfgang CL. Revisions of international consensus Fukuoka guidelines for the management of IPMN of the pancreas. *Pancreatology* 2017; **17**: 738-753 [PMID: 28735806 DOI: 10.1016/j.pan.2017.07.007]

12 **Tsukagoshi M**, Araki K, Saito F, Kubo N, Watanabe A, Igarashi T, Ishii N, Yamanaka T, Shirabe K, Kuwano H. Evaluation of the International Consensus Guidelines for the Surgical Resection of Intraductal Papillary Mucinous Neoplasms. *Dig Dis Sci* 2018; **63**: 860-867 [PMID: 28667432 DOI: 10.1007/s10620-017-4667-y]

13 **Sugimoto M**, Elliott IA, Nguyen AH, Kim S, Muthusamy VR, Watson R, Hines OJ, Dawson DW, Reber HA, Donahue TR. Assessment of a Revised Management Strategy for Patients With Intraductal Papillary Mucinous Neoplasms Involving the Main Pancreatic Duct. *JAMA Surg* 2017; **152**: e163349 [PMID: 27829085 DOI: 10.1001/jamasurg.2016.3349]

14 **Yamada S**, Fujii T, Murotani K, Kanda M, Sugimoto H, Nakayama G, Koike M, Fujiwara M, Nakao A, Kodera Y. Comparison of the international consensus guidelines for predicting malignancy in intraductal papillary mucinous neoplasms. *Surgery* 2016; **159**: 878-884 [PMID: 26506564 DOI: 10.1016/j.surg.2015.08.042]

15 **Heckler M**, Michalski CW, Schaefle S, Kaiser J, Büchler MW, Hackert T. The Sendai and Fukuoka consensus criteria for the management of branch duct IPMN - A meta-analysis on their accuracy. *Pancreatology* 2017; **17**: 255-262 [PMID: 28189431 DOI: 10.1016/j.pan.2017.01.011]

16 **Robles EP**, Maire F, Cros J, Vullierme MP, Rebours V, Sauvanet A, Aubert A, Dokmak S, Lévy P, Ruszniewski P. Accuracy of 2012 International Consensus Guidelines for the prediction of malignancy of branch-duct intraductal papillary mucinous neoplasms of the pancreas. *United European Gastroenterol J* 2016; **4**: 580-586 [PMID: 27536368 DOI: 10.1177/2050640615623370]

17 **de Pretis N**, Mukewar S, Aryal-Khanal A, Bi Y, Takahashi N, Chari S. Pancreatic cysts: Diagnostic accuracy and risk of inappropriate resections. *Pancreatology* 2017; **17**: 267-272 [PMID: 28117220 DOI: 10.1016/j.pan.2017.01.002]

18 **Kumar V**, Gu Y, Basu S, Berglund A, Eschrich SA, Schabath MB, Forster K, Aerts HJ, Dekker A, Fenstermacher D, Goldgof DB, Hall LO, Lambin P, Balagurunathan Y, Gatenby RA, Gillies RJ. Radiomics: the process and the challenges. *Magn Reson Imaging* 2012; **30**: 1234-1248 [PMID: 22898692 DOI: 10.1016/j.mri.2012.06.010]

19 **Gatenby RA**, Grove O, Gillies RJ. Quantitative imaging in cancer evolution and ecology. *Radiology* 2013; **269**: 8-15 [PMID: 24062559 DOI: 10.1148/radiol.13122697]

20 **Grove O**, Berglund AE, Schabath MB, Aerts HJ, Dekker A, Wang H, Velazquez ER, Lambin P, Gu Y, Balagurunathan Y, Eikman E, Gatenby RA, Eschrich S, Gillies RJ. Quantitative computed tomographic descriptors associate tumor shape complexity and intratumor heterogeneity with prognosis in lung adenocarcinoma. *PLoS One* 2015; **10**: e0118261 [PMID: 25739030 DOI: 10.1371/journal.pone.0118261]

21 **Balagurunathan Y**, Gu Y, Wang H, Kumar V, Grove O, Hawkins S, Kim J, Goldgof DB, Hall LO, Gatenby RA, Gillies RJ. Reproducibility and Prognosis of Quantitative Features Extracted from CT Images. *Transl Oncol* 2014; **7**: 72-87 [PMID: 24772210 DOI: 10.1593/tlo.13844]

22 **Fave X**, Mackin D, Yang J, Zhang J, Fried D, Balter P, Followill D, Gomez D, Jones AK, Stingo F, Fontenot J, Court L. Can radiomics features be reproducibly measured from CBCT images for patients with non-small cell lung cancer? *Med Phys* 2015; **42**: 6784-6797 [PMID: 26632036 DOI: 10.1118/1.4934826]

23 **Leijenaar RT**, Carvalho S, Velazquez ER, van Elmpt WJ, Parmar C, Hoekstra OS, Hoekstra CJ, Boellaard R, Dekker AL, Gillies RJ, Aerts HJ, Lambin P. Stability of FDG-PET Radiomics features: an integrated analysis of test-retest and inter-observer variability. *Acta Oncol* 2013; **52**: 1391-1397 [PMID: 24047337 DOI: 10.1109/ACCESS.2019.2923755]

24 **Peerlings J**, Woodruff HC, Winfield JM, Ibrahim A, Van Beers BE, Heerschap A, Jackson A, Wildberger JE, Mottaghy FM, DeSouza NM, Lambin P. Stability of radiomics features in apparent diffusion coefficient maps from a multi-centre test-retest trial. *Sci Rep* 2019; **9**: 4800 [PMID: 30886309 DOI: 10.1038/s41598-019-41344-5]

25 **Qiu Q**, Duan J, Duan Z, Meng X, Ma C, Zhu J, Lu J, Liu T, Yin Y. Reproducibility and non-redundancy of radiomic features extracted from arterial phase CT scans in hepatocellular carcinoma patients: impact of tumor segmentation variability. *Quant Imaging Med Surg* 2019; **9**: 453-464 [PMID: 31032192 DOI: 10.21037/qims.2019.03.02]

26 **Coroller TP**, Grossmann P, Hou Y, Rios Velazquez E, Leijenaar RT, Hermann G, Lambin P, Haibe-Kains B, Mak RH, Aerts HJ. CT-based radiomic signature predicts distant metastasis in lung adenocarcinoma. *Radiother Oncol* 2015; **114**: 345-350 [PMID: 25746350 DOI: 10.1016/j.radonc.2015.02.015]

27 **Grossmann P**, Narayan V, Chang K, Rahman R, Abrey L, Reardon DA, Schwartz LH, Wen PY, Alexander BM, Huang R, Aerts HJWL. Quantitative imaging biomarkers for risk stratification of patients with recurrent glioblastoma treated with bevacizumab. *Neuro Oncol* 2017; **19**: 1688-1697 [PMID: 28499022 DOI: 10.1093/neuonc/nox092]

28 **Koo HJ**, Sung YS, Shim WH, Xu H, Choi CM, Kim HR, Lee JB, Kim MY. Quantitative Computed Tomography Features for Predicting Tumor Recurrence in Patients with Surgically Resected Adenocarcinoma of the Lung. *PLoS One* 2017; **12**: e0167955 [PMID: 28068363 DOI: 10.1371/journal.pone.0167955]

29 **Ou D**, Blanchard P, Rosellini S, Levy A, Nguyen F, Leijenaar RTH, Garberis I, Gorphe P, Bidault F, Ferté C, Robert C, Casiraghi O, Scoazec JY, Lambin P, Temam S, Deutsch E, Tao Y. Predictive and prognostic value of CT based radiomics signature in locally advanced head and neck cancers patients treated with concurrent chemoradiotherapy or bioradiotherapy and its added value to Human Papillomavirus status. *Oral Oncol* 2017; **71**: 150-155 [PMID: 28688683 DOI: 10.1016/j.oraloncology.2017.06.015]

30 **Yu W**, Tang C, Hobbs BP, Li X, Koay EJ, Wistuba II, Sepesi B, Behrens C, Rodriguez Canales J, Parra Cuentas ER, Erasmus JJ, Court LE, Chang JY. Development and Validation of a Predictive Radiomics Model for Clinical Outcomes in Stage I Non-small Cell Lung Cancer. *Int J Radiat Oncol Biol Phys* 2018; **102**: 1090-1097 [PMID: 29246722 DOI: 10.1016/j.ijrobp.2017.10.046]

31 **Lee HJ**, Kim MJ, Choi JY, Hong HS, Kim KA. Relative accuracy of CT and MRI in the differentiation of benign from malignant pancreatic cystic lesions. *Clin Radiol* 2011; **66**: 315-321 [PMID: 21356393 DOI: 10.1016/j.crad.2010.06.019]

32 **Sainani NI**, Saokar A, Deshpande V, Fernández-del Castillo C, Hahn P, Sahani DV. Comparative performance of MDCT and MRI with MR cholangiopancreatography in characterizing small pancreatic cysts. *AJR Am J Roentgenol* 2009; **193**: 722-731 [PMID: 19696285 DOI: 10.2214/AJR.08.1253]

33 **Permuth JB**, Choi J, Balarunathan Y, Kim J, Chen DT, Chen L, Orcutt S, Doepker MP, Gage K, Zhang G, Latifi K, Hoffe S, Jiang K, Coppola D, Centeno BA, Magliocco A, Li Q, Trevino J, Merchant N, Gillies R, Malafa M; Florida Pancreas Collaborative. Combining radiomic features with a miRNA classifier may improve prediction of malignant pathology for pancreatic intraductal papillary mucinous neoplasms. *Oncotarget* 2016; **7**: 85785-85797 [PMID: 27589689 DOI: 10.18632/oncotarget.11768]

34 **Hanania AN**, Bantis LE, Feng Z, Wang H, Tamm EP, Katz MH, Maitra A, Koay EJ. Quantitative imaging to evaluate malignant potential of IPMNs. *Oncotarget* 2016; **7**: 85776-85784 [PMID: 27588410 DOI: 10.18632/oncotarget.11769]

35 **Chakraborty J**, Midya A, Gazit L, Attiyeh M, Langdon-Embry L, Allen PJ, Do RKG, Simpson AL. CT radiomics to predict high-risk intraductal papillary mucinous neoplasms of the pancreas. *Med Phys* 2018; **45**: 5019-5029 [PMID: 30176047 DOI: 10.1002/mp.13159]

36 **Ganeshan B**, Abaleke S, Young RC, Chatwin CR, Miles KA. Texture analysis of non-small cell lung cancer on unenhanced computed tomography: initial evidence for a relationship with tumour glucose metabolism and stage. *Cancer Imaging* 2010; **10**: 137-143 [PMID: 20605762 DOI: 10.1102/1470-7330.2010.0021]

37 **Ganeshan B**, Panayiotou E, Burnand K, Dizdarevic S, Miles K. Tumour heterogeneity in non-small cell lung carcinoma assessed by CT texture analysis: a potential marker of survival. *Eur Radiol* 2012; **22**: 796-802 [PMID: 22086561 DOI: 10.1007/s00330-011-2319-8]

38 **Ganeshan B**, Skogen K, Pressney I, Coutroubis D, Miles K. Tumour heterogeneity in oesophageal cancer assessed by CT texture analysis: preliminary evidence of an association with tumour metabolism, stage, and survival. *Clin Radiol* 2012; **67**: 157-164 [PMID: 21943720 DOI: 10.1016/j.crad.2011.08.012]

39 **Ng F**, Ganeshan B, Kozarski R, Miles KA, Goh V. Assessment of primary colorectal cancer heterogeneity by using whole-tumor texture analysis: contrast-enhanced CT texture as a biomarker of 5-year survival. *Radiology* 2013; **266**: 177-184 [PMID: 23151829 DOI: 10.1148/radiol.12120254]

40 **Yip C**, Landau D, Kozarski R, Ganeshan B, Thomas R, Michaelidou A, Goh V. Primary esophageal cancer: heterogeneity as potential prognostic biomarker in patients treated with definitive chemotherapy and radiation therapy. *Radiology* 2014; **270**: 141-148 [PMID: 23985274 DOI: 10.1148/radiol.13122869]

41 **Zhang H**, Graham CM, Elci O, Griswold ME, Zhang X, Khan MA, Pitman K, Caudell JJ, Hamilton RD, Ganeshan B, Smith AD. Locally advanced squamous cell carcinoma of the head and neck: CT texture and histogram analysis allow independent prediction of overall survival in patients treated with induction chemotherapy. *Radiology* 2013; **269**: 801-809 [PMID: 23912620 DOI: 10.1148/radiol.13130110]

42 **Burrell RA**, McGranahan N, Bartek J, Swanton C. The causes and consequences of genetic heterogeneity in cancer evolution. *Nature* 2013; **501**: 338-345 [PMID: 24048066 DOI: 10.1038/nature12625]

43 **Caswell DR**, Swanton C. The role of tumour heterogeneity and clonal cooperativity in metastasis, immune evasion and clinical outcome. *BMC Med* 2017; **15**: 133 [PMID: 28716075 DOI: 10.1186/s12916-017-0900-y]

44 **Dagogo-Jack I**, Shaw AT. Tumour heterogeneity and resistance to cancer therapies. *Nat Rev Clin Oncol* 2018; **15**: 81-94 [PMID: 29115304 DOI: 10.1038/nrclinonc.2017.166]

45 **Marusyk A**, Almendro V, Polyak K. Intra-tumour heterogeneity: a looking glass for cancer? *Nat Rev*

Cancer 2012; **12**: 323-334 [PMID: 22513401 DOI: 10.1038/nrc3261]
46 **Brouwer A**, De Laere B, Peeters D, Peeters M, Salgado R, Dirix L, Van Laere S. Evaluation and consequences of heterogeneity in the circulating tumor cell compartment. *Oncotarget* 2016; **7**: 48625-48643 [PMID: 26980749 DOI: 10.18632/oncotarget.8015]
47 **Bae KT**. Intravenous contrast medium administration and scan timing at CT: considerations and approaches. *Radiology* 2010; **256**: 32-61 [PMID: 20574084 DOI: 10.1148/radiol.10090908]
48 **Tunali I**, Gray JE, Qi J, Abdalah M, Jeong DK, Guvenis A, Gillies RJ, Schabath MB. Novel clinical and radiomic predictors of rapid disease progression phenotypes among lung cancer patients treated with immunotherapy: An early report. *Lung Cancer* 2019; **129**: 75-79 [PMID: 30797495 DOI: 10.1016/j.lungcan.2019.01.010]
49 **Shafiq-Ul-Hassan M**, Zhang GG, Latifi K, Ullah G, Hunt DC, Balagurunathan Y, Abdalah MA, Schabath MB, Goldgof DG, Mackin D, Court LE, Gillies RJ, Moros EG. Intrinsic dependencies of CT radiomic features on voxel size and number of gray levels. *Med Phys* 2017; **44**: 1050-1062 [PMID: 28112418 DOI: 10.1002/mp.12123]
50 **Mackin D**, Fave X, Zhang L, Yang J, Jones AK, Ng CS, Court L. Harmonizing the pixel size in retrospective computed tomography radiomics studies. *PLoS One* 2017; **12**: e0178524 [PMID: 28934225 DOI: 10.1371/journal.pone.0178524]
51 **Pagliari D**, Saviano A, Serricchio ML, Dal Lago AA, Brizi MG, Lanza F, Manfredi R, Gasbarrini A, Attili F. Uptodate in the assessment and management of intraductal papillary mucinous neoplasms of the pancreas. *Eur Rev Med Pharmacol Sci* 2017; **21**: 2858-2874 [PMID: 28682431]

Published by Baishideng Publishing Group Inc
7041 Koll Center Parkway, Suite 160, Pleasanton, CA 94566, USA
Telephone: +1-925-3991568
E-mail: bpgoffice@wjgnet.com
Help Desk:http://www.f6publishing.com/helpdesk
http://www.wjgnet.com